AD-A068 107 AIL DEER PARK N Y F/G 14/2
STAFF RADIOMETRIC SENSOR.(U)
FEB 79 DAAK10-78-C-0085
UNCLASSIFIED AIL-FTR-1 NL

1 OF 1
ADA
068107

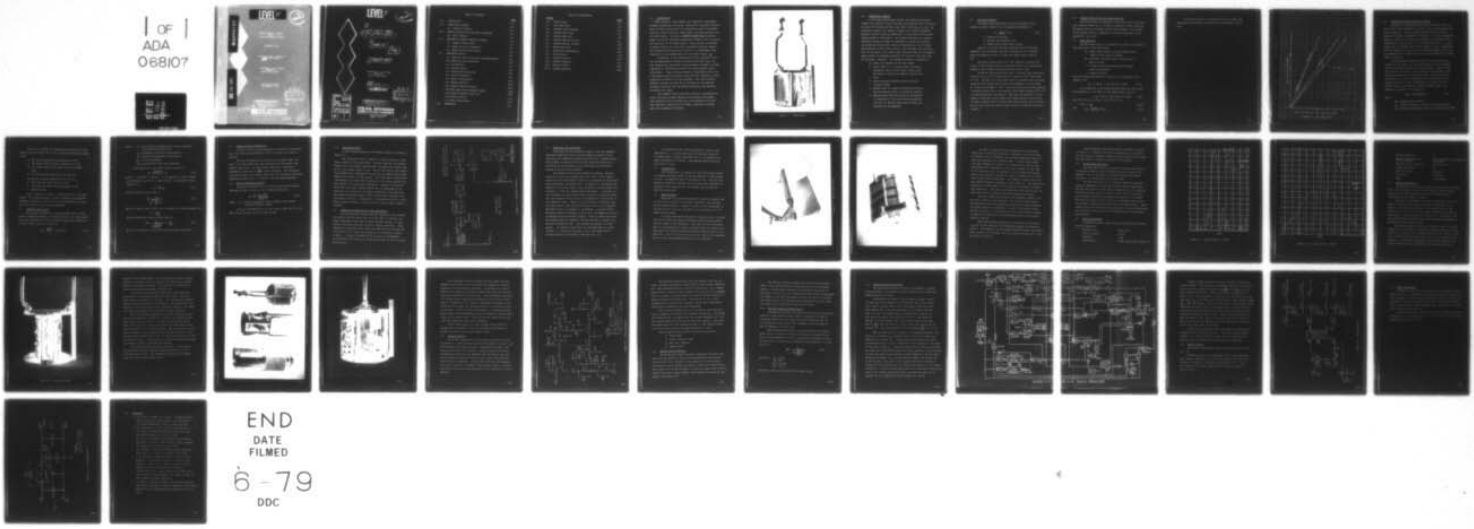

END
DATE
FILMED
6-79
DDC

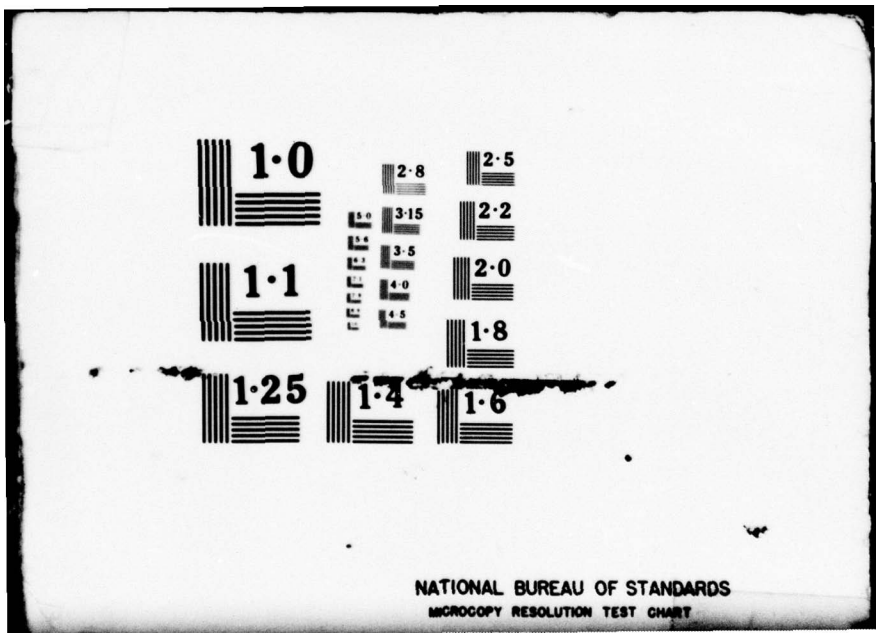
1·0
1·1
1·25
2·8
3·15
3·5
4·0
4·5
2·5
2·2
2·0
1·8
1·4
1·6
NATIONAL BUREAU OF STANDARDS
MICROCOPY RESOLUTION TEST CHART

LEVEL II

2

FINAL TECHNICAL REPORT FOR STAFF RADIOMETRIC SENSOR

FEBRUARY 1979

Provided Under Contract
[redacted]10-78-C-0085

Department of the Army
ARRADCOM
Dover, New Jersey

AIL Report FTR-1
AIL Project D549

LEVEL II

(2)

(9)

FINAL TECHNICAL REPORT
FOR
STAFF RADIOMETRIC SENSOR

(6)

(11) FEBRUARY 1979

(12) 42p.

Provided Under Contract

(15) DAAK10-78-C-0085

Department of the Army
ARRADCOM
Dover, New Jersey

(14) AIL Report-FTR-1
AIL Project D549

DDC
RECEIVED
MAY 2 1979
D

ACCESSION for	
DTIC	White Section X
DDC	Buff Section ☐
UNANNOUNCED	☐
JUSTIFICATION	
Per Ltr. on File	
BY	
DISTRIBUTION/AVAILABILITY CODES	
Dist.	AVAIL. and/or SPECIAL
A	

DISTRIBUTION STATEMENT A
Approved for public release;
Distribution Unlimited

AIL DIVISION
CUTLER-HAMMER
DEER PARK, LONG ISLAND, NEW YORK 11729

404967

(B)

TABLE OF CONTENTS

LIST OF ILLUSTRATIONS

1.0 INTRODUCTION

AIL Division, Cutler-Hammer has conducted a development program encompassing the design, fabrication, laboratory testing, field testing, and delivery of a radiometric sensor (including receiver, signal processor, power supply, and dual antennas) for the STAFF system. This sensor ~~shown in Figure 1~~ includes a number of new and innovative approaches devised by AIL to achieve the objectives of the STAFF system. These include a technique to measure sensor spin rate and a radiometric antenna temperature summation technique which results in a considerable simplification in the implementation of the STAFF concept.

In addition to the specialized circuits designed by AIL for the measurement of sensor orientation and spin rate, AIL also designed and fabricated high performance microwave (35 GHz) components to specifically satisfy the STAFF system's unique requirements. These include antennas, a proprietary mixer, and a customized waveguide assembly that sums the radiometric noise components provided by the two antennas. This noise summing assembly obviates the need for an RF switch or two separate microwave receivers thus increasing reliability and lowering potential unit costs.

The complete STAFF sensor was hardened to withstand the severe firing and flight mechanical and thermal environment. The completed sensor including all of its hardened structure and components weighed only 3.6 pounds, although its design goal was a maximum of 8 pounds.

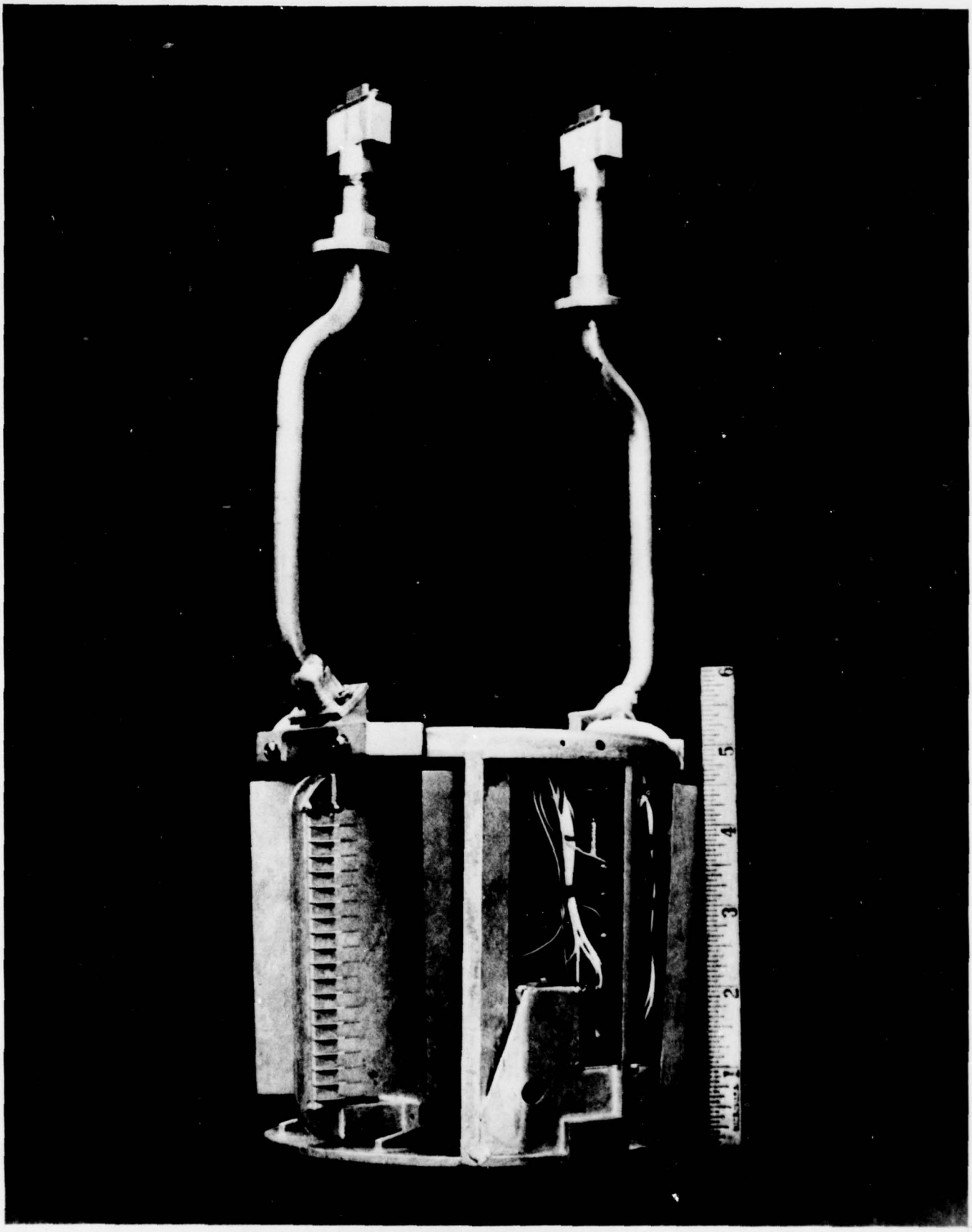

Figure 1-1. STAFF Sensor

2.0 OPERATIONAL SCENARIO

In the STAFF operational concept, the rotating projectile travels at a nominal 25 meter (82 feet) altitude and with a velocity of about 1000 ft/sec, and has a spin rate of 100 rps $\pm$ 15 rps. The projectile contains two nominal 7 degree (0.12 radian) beamwidth antennas oriented nearly perpendicular to the velocity vector with viewing angles of 180° apart. The antennas are part of a 35 GHz radiometer system designed and optimized to detect the presence of an armored vehicle whose nominal dimensions are 10 by 20 feet. The projectile's fire control system, upon detection and verification of the target, will launch armor piercing slugs at the target's upper surface via warheads displaced 90° along the spin axis from the antennas' boresight. The radiometer system is designed to:

1) Detect the presence of the tank target
2) Verify that it is a proper target by placing acceptance limits on the target signal level and duration within the antenna's ground footprint
3) Clear the proper warhead cover by firing a thruster charge
4) Require that the target be detected by each of the two antennas during 1 projectile rotation
5) Appropriately delay the firing of the warhead to compensate for the electronics processing time and the angular displacement between the antennas and the warheads

2.1 Footprint Geometry

The STAFF system parameters places the antenna's 3-dB (nearly circular) footprint on the ground with diameter D

$$D = \frac{h}{\cos \theta} \tan \alpha \qquad (2\text{-}1)$$

h = projectile altitude

α = antenna 3-dB beamwidth (7°)

θ = target vector angle from vertical

Thus for a 25 meter (82 feet) altitude and a 7° antenna beamwidth, the 3-dB ground footprint diameter is 10 ft directly below the projectile and 14 ft when the target vector angle is 45°.

The ground target velocity of the footprint is nearly 10^3 ft/sec in the forward direction and $2\pi\omega H \sec^2 \theta$ in the cross-track direction with ω being the projectile spin rate in rps.

At the 82 foot altitude and with ω = 100 rps, the cross-track velocity is 51.5×10^3 ft/sec with $\theta = 0$ and 103×10^3 ft/sec when $\theta = 45^{\circ}$. Obviously the cross-track velocity dominates and the ground footprint will travel (cross-track) one footprint in 0.19 ms when $\theta = 0$ and 0.14 ms when $\theta = 45^{\circ}$. Since the 100 rps spin rate produces 1 revolution each 10 ms, the footprint will travel forward $10^{-2} \times 10^3$ = 10 feet during each revolution. Thus with two antennas, a 5-foot forward travel will occur between each ground antenna scan, and it is highly probable that a 10-foot tank target (worst case condition) will be well within the beam of each of the two antennas during one rotation.

3.0 TARGET LOCATION WITH SPIN RATE VARIATION

The STAFF sensor is required to detect and locate the center of an armored target and to initiate an explosive output signal at the proper time to the proper double ended warhead. The accuracy of the warhead aiming is dependent on accurate knowledge of the projectile's spin rate.

3.1 Error Analysis

The SFF impact point on the ground is D_F feet to the side of the projectile's flight path when:

θ_o = angle from vertical of sensor antenna boresight at time target is sensed

θ_F = munitions boresight angle from vertical at time of firing

T = firing time delay between sensing target and firing warhead

h = sensor altitude

When the antenna and munitions boresights are displaced by $\pi/2$ radians, then

$$D_F = h \tan \theta_F = h \tan (\theta_o - \pi/2 + 2\pi\omega T) \qquad (3\text{-}1)$$

An uncertainty in the projectile spin rate, $\Delta\omega$, will cause an uncertainty in the offset of the impact point, ΔD_F, of:

$$\Delta D_F = 2\pi T h \, \Delta\omega \sec^2 (\theta_o - \pi/2 + 2\pi\omega T) \qquad (3\text{-}2)$$

and there will be no error in D_F if $2\pi\omega T = \pi/2$.

Then $$T = \frac{1}{4\omega} \qquad (3\text{-}3)$$

and $$\Delta D_F = \frac{h\pi}{2} \frac{\Delta\omega}{\omega} \sec^2 \theta_o \qquad (3\text{-}4)$$

This error equation is plotted in Figure 3-1 where the importance of minimizing the rotation rate uncertainty can be seen.

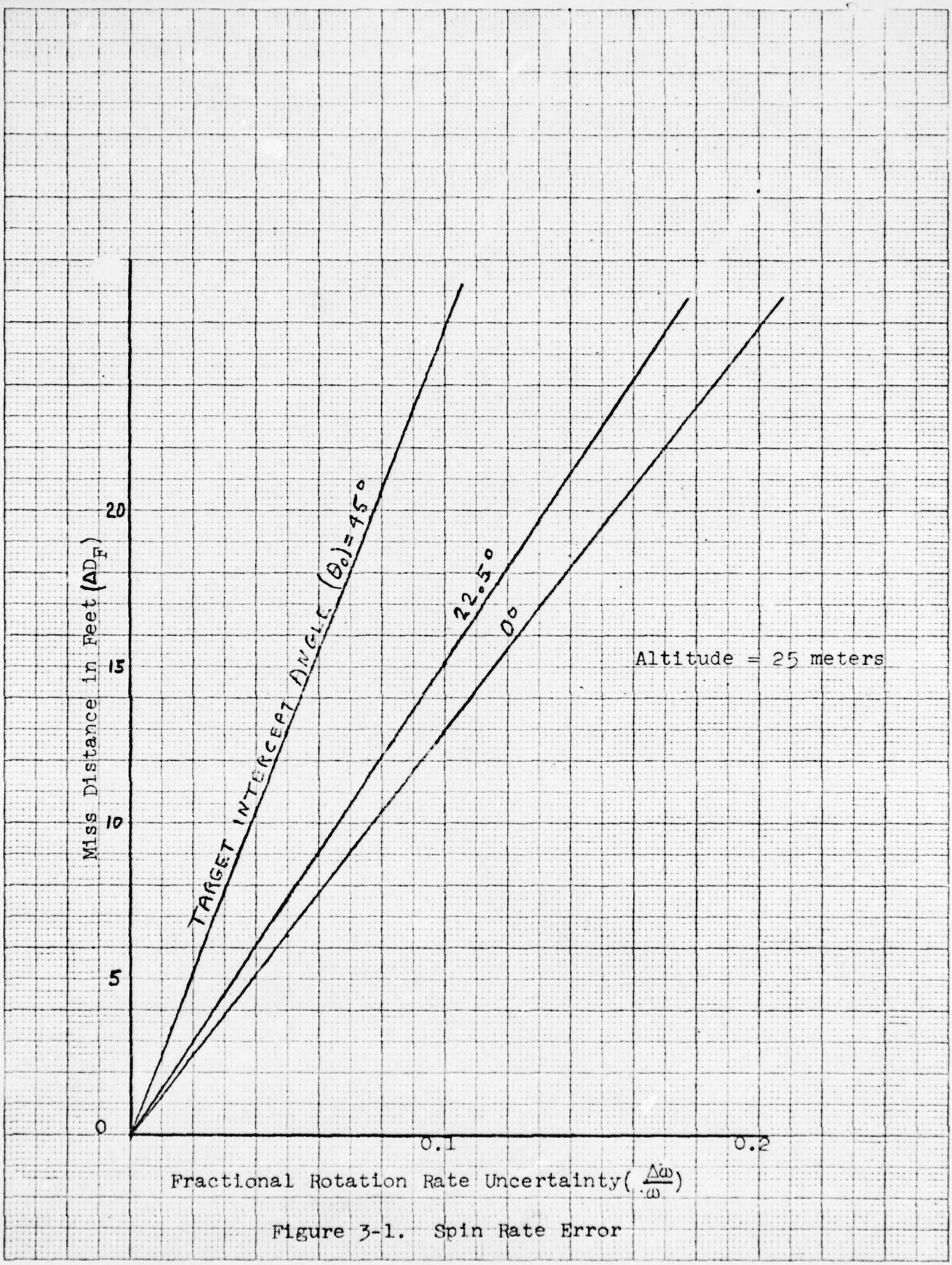

Figure 3-1. Spin Rate Error

4.0 RADIOMETRIC TARGET DETECTION CRITERIA

Detection of an armored vehicle with the STAFF sensor is due to the 35 GHz radiometric contrast of the vehicle against the earth background. A metal surface viewed from above tends to assume a radiometric temperature determined by the sky temperature which it reflects, while the earth appears as a blackbody with a temperature of about 270K[1]. In accordance with Ref. 1, we may assume that the armored vehicle will appear to have a temperature of about 60K when it beam-fills the observing antenna, while the sky temperature will vary between 10K and 100K depending on atmospheric conditions.

The brightness temperature sensed by an antenna is the integral of the product of its antenna pattern and the temperature profile present across the entire pattern. Thus the beam efficiency of the antenna (which defines the percentage of the total energy received by an antenna within its main beam when surrounded by a constant temperature blackbody) should be as high as possible in order to maximize the contrast due to a metallic target being within a scanning antenna beam. The temperature sensed by the antenna is:

$$T_{AV} + (1-M_B)(T_B-T_{AV}) \qquad (4\text{-}1)$$

where:

M_B = antenna beam efficiency

T_{AV} = average temperature within the antenna mainlobe

T_B = background temperature seen by the antenna sidelobes

In order to estimate the temperature contrast due to the armored vehicle we make use of the following conservative assumptions:

1) The ground radiometric temperature is 270K.
2) The armored vehicle target temperature is 70K.
3) The armored vehicle only half fills the antenna beam.
4) The antenna beam efficiency is 80 percent.

The apparent antenna temperature will then be:

1) 270K when the target is not in view
2) 142K when the target fills 80 percent of the efficient beam

Thus a contrast of 270-142 = 128K exists due to the tank target. This expected target contrast determines the required radiometer temperature sensitivity for a given detection probability as shown in the following paragraph.

4.1 SIGNAL TO NOISE RATIO

The signal-to-noise ratio (SNR) associated with a noise summing radiometer approach is developed below. The total apparent noise temperature (including receiver generated) referred to a hybrid output sum port is given by:

$$T_{op} = \frac{T_A+T_B}{2} + (F_R-1)\,290 \qquad (4\text{-}2)$$

where: F_R = system double sideband noise figure referenced to a hybrid output sum port

T_A = brightness temperature from antenna 1

T_B = brightness temperature from antenna 2

B_{IF} = IF noise bandwidth

B_N = postdetection video noise bandwidth

The postdetection rms noise voltage is given by

$$V_N = \sqrt{2B_N B_{IF}}\, k\, T_{op} \tag{4-3}$$

where k = Boltzmann's constant. If T_A changes by a small temperature increment, T_s, due to a target signal, the resultant signal voltage S is:

$$S = k \frac{T_s}{2} B_{IF} \tag{4-4}$$

and the signal-to-noise ratio is

$$\frac{S}{N} = \frac{T_s}{\sqrt{8 \frac{B_N}{B_{IF}}}\, T_{op}} \tag{4-5}$$

When the lowpass video filter is an RC network with time constant, then

$$(T = \frac{1}{4B_N})$$

then the radiometer signal-to-noise ratio is

$$SNR = \frac{T_s}{T_{op}\sqrt{\frac{2}{B_{IF}T}}}, \quad T = \frac{1}{4B_N} \tag{4-6}$$

which is the relation for an ideal Dicke switched radiometer.

4.2 Target Detection Probability

In order to have a high probability of detection (99 percent) and a low false alarm probability (10^{-6}) a SNR of 7.1 (17 dB) is required.

The SNR is determined by the ratio of the 128K target contrast to the equivalent rms noise fluctuation or radiometer temperature sensitivity. For the stated conditions, a radiometer temperature sensitivity of $\frac{128}{7.1} = 18K$ is required. The corresponding sensor system noise figure, based upon the calculated radiometer temperature sensitivity, is treated in the following paragraph.

4.3 Sensor System Noise Figure

The noise fluctuation ΔT in a Dicke switch double sideband radiometer system is given by the following expression:

$$\Delta T = \sqrt{2}\ \frac{F_s \times 290}{\sqrt{B_{IF}\ T}} \qquad (4\text{-}7)$$

where: F_s = overall radiometer double sideband noise figure (including antenna losses)

If B_{IF} is 500 MHz and T = 0.1 ms, then in order for ΔT to be 18K or less, F_s must be 9.8 (10 dB) or less.

5.0 RADIOMETER DESIGN

A block diagram showing the radiometer receiver is shown in Figure 5-1.

The 3-dB hybrid shown in Figure 5-1 has the ability to sum powers present at its input ports. However, when two non-coherent signals are being summed, thermodynamic considerations require that half of each signal power be lost. Thus if the hybrid input powers are associated with temperatures T_A and T_B, the summed output temperature will appear to be $\frac{1}{2}(T_A+T_B)$. This 3-dB loss in sensitivity corresponds to the sensitivity degradation of a Dicke switched system compared to a total power radiometer. However, it should be noted that this hybrid summing system has the advantages of not requiring an RF switch nor the added complexity of the Dicke system signal processing (switch driver, switch rate oscillator, and synchronous detector). Furthermore, a considerable saving in size, weight, power consumption, and cost of the overall sensor system is achieved.

5.1 Direction Sensing and Spin Rate Measurement

As the projectile rotates with each antenna in turn viewing the sky and then the earth, each for about 180° of rotation, the summed temperature will tend to remain constant (except for temperature transients which will occur at horizon crossings). These temperature transients occur during the time when the antennas are viewing the horizon where the probability of destroying a target is small. It should be noted that the firing of the armaments is inhibited in the vicinity of the horizons with no loss in system effectiveness.

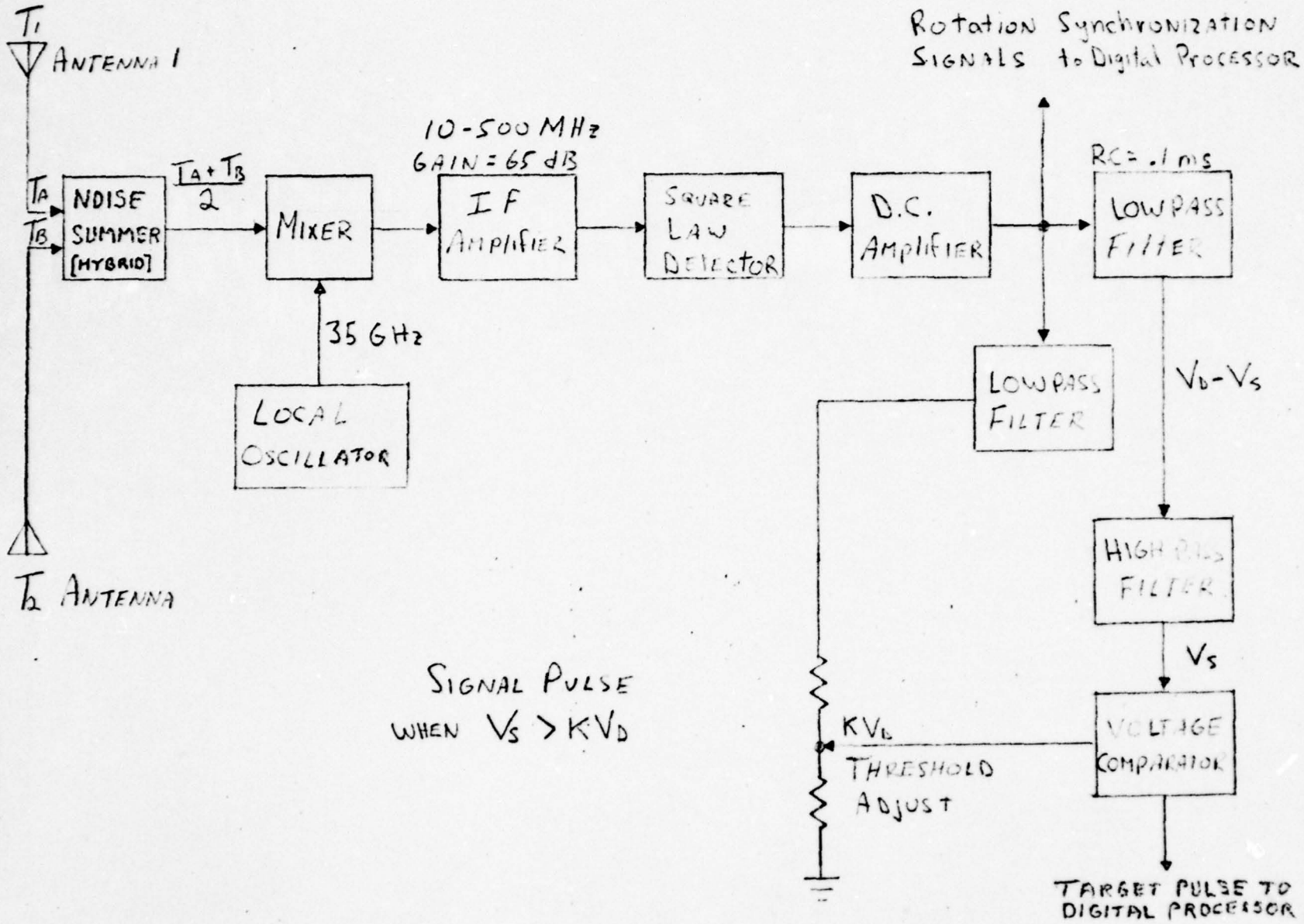

Figure 5-1. Radiometer Receiver

5.2 Mixer and Gunn Oscillator

A key part of the radiometric sensor is the AIL designed balanced 35-GHz mixer which utilizes advanced printed circuit technology for potential minimum production cost. Further potential economy is achieved with low-cost beam-lead diodes and a thin-film pad which promotes local oscillator (LO) stability without a costly ferrite isolator.

The printed circuit mixer combines microstrip, coplanar line and fin-line on a single board (Ref. 3-5). The LO signal enters the mixer and passes through an LO pad which is constructed from a metal-film resistance card. In addition to increasing the stability of the Gunn device local oscillator, the pad reduces the LO drive to 9 dBm, for optimum mixer performance. A printed circuit monopole on a Duroid-5880 board provides the required transition to microstrip which excites the coplanar-line diode mount in the unbalanced mode. Inherent RF/LO isolation is obtained since the diode mount is fed from the fin-line RF port in the balanced mode which does not propagate in microstrip. A printed circuit matching network is provided at the RF port for compatibility with a standard UG-559/U waveguide flange. A pair of beam-lead diodes are bonded across the coplanar line and returned to ground at dc through LO-blocking stubs. This permits the diodes to be self biased. It should be noted that the described mixer is a modification of the device utilized by AIL in the STAFF Phase I program radiometer delivered to ARRADCOM (Ref. 6,7).

A miniaturized Gunn device oscillator is used as the radiometer LO. It is the same type GDO that was chosen for the STAFF Phase I program radiometer due to its inherent low power requirement of 0.8 watt. The measured mixer/LO conversion loss is 7.8 dB.

5 3 IF Amplifier

The IF amplifier is composed of thin-film devices having a frequency response between 10 and 500 MHz with a noise figure of 4 dB. The amplifier gain is nominally 65 dB. This gain and bandwidth combination assures that the noise power presented to the tunnel diode detector will be suitable ($\approx$ -20 dBm) for sensitive processing.

5.4 Sensor Antenna

The array fed cylindrical parabolic reflector antenna used in this sensor consists of two major components; the reflector and the waveguide array. Figures 5-2 and 5-3 are photographs of the antenna which has been developed at AIL especially for the STAFF sensor program.

A slotted rectangular waveguide is mounted within the focal line of a cylindrical parabolic antenna reflector which extends the full length of the waveguide. Slots are cut into one narrow wall of the waveguide at regular intervals along its length, with alternate slots inclined at opposite angles perpendicular to the waveguide. Beyond the slotted section, both ends of the waveguide are bent back to facilitate mounting to the reflector.

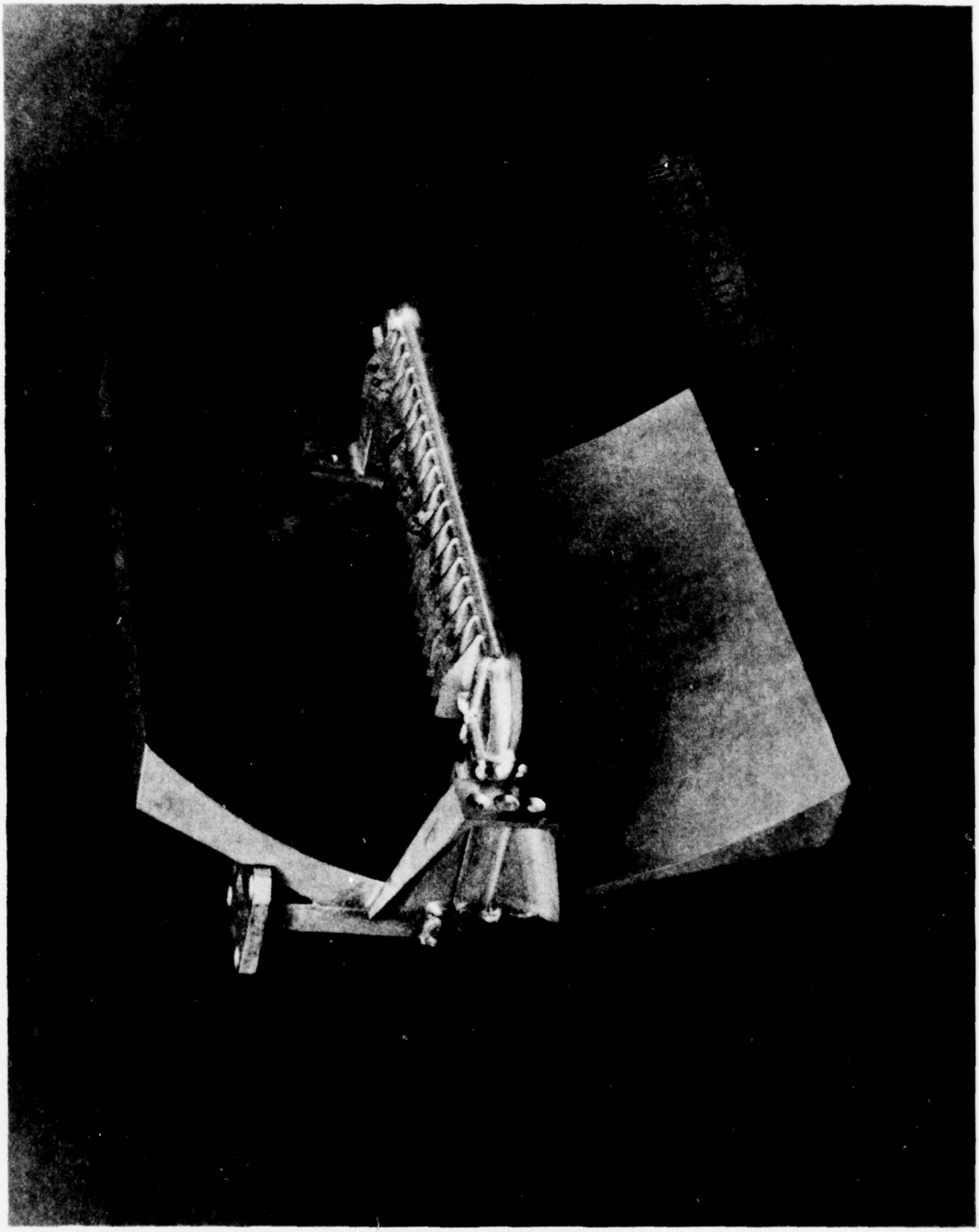

Figure 5-2. Antenna Front View

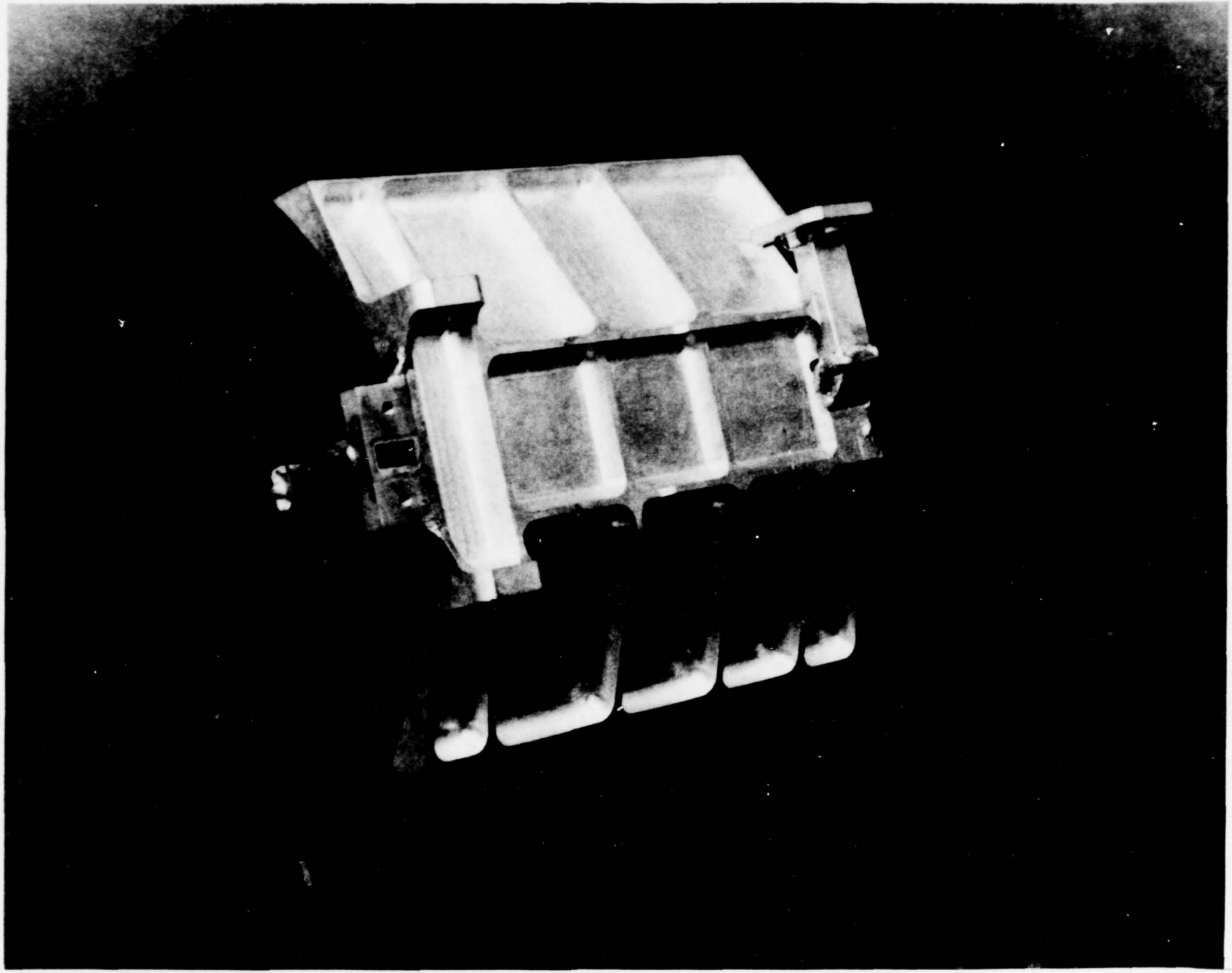

Figure 5-3. Antenna Rear View

In order to provide sufficient bandwidth, the proposed design uses a traveling wave array. Therefore, an end-fed array of resonant slots is spaced at non-resonant separations along the guide and terminated in a matched load. A finite squint angle (the angle between the normal of the array and the line of maximum radiation) is inherent in this type of array; in this case, a 7.5° angle was used. In addition, a $\pm 2.5^{\circ}$ mechanical adjustment of the antenna is provided in order to satisfy the 5° to 10° squint angle system requirement. The change in squint angle over the operating range of frequency is less than 2.5°. The electrical properties of each element in the array are controlled by mechanical dimensions. The proper inclination and slot length along the array were found by computer-aided and experimental design.

The slots behave electrically like radiating elements that are shunt-coupled to the waveguide. The coupling varies along the waveguide producing an amplitude distribution which satisfies the proper reflector illumination to obtain the desired E-plane radiation patterns. Each successive slot is fed in phase reversal to reduce slot spacing and to avoid grating lobes in the E-plane radiation pattern.

The H-plane radiation pattern is controlled by the reflector size in this plane and the illumination across the parabolic profile. The sidelobes in the H-plane radiation pattern are higher than obtained in the E-plane, since the array obscures part of the cylindrical reflector.

Typical measured radiation patterns are shown in Figures 5-4 and 5-5. A matched load, which absorbes about 5 percent of the input power, eliminates reflections from the end of the array and thus prevents unwanted sidelobes in the E-plane.

5.5 Antenna Beam Efficiency

The beam efficiency of an antenna is defined as the ratio of the power radiated within the main beam to the total power radiated. All of the power of an ideal antenna (100 percent efficiency) is radiated within the main beam.

The beam efficiency of a cylindrical parabolic reflector system is dependent upon both the reflector and the feed array. The efficiency factor of the feed is determined by (1) the amount of energy spilled over the reflector edges, and (2) the energy lost by phase errors due to mechanical tolerances in the array. The efficiency factor of the reflector is dependent mainly upon the surface roughness and deviation from the ideal contour. Using careful design and high precision numerically controlled manufacturing techniques, efficiencies in the lower 80 percent region have been realized.

5.6 Antenna Parameters

The following design goals have been established as minimum antenna parameters:

Aperture size:	< 3.5 inch^2
Center frequency:	35 GHz
Bandwidth:	1 GHz
Polarization:	Linear along flight direction

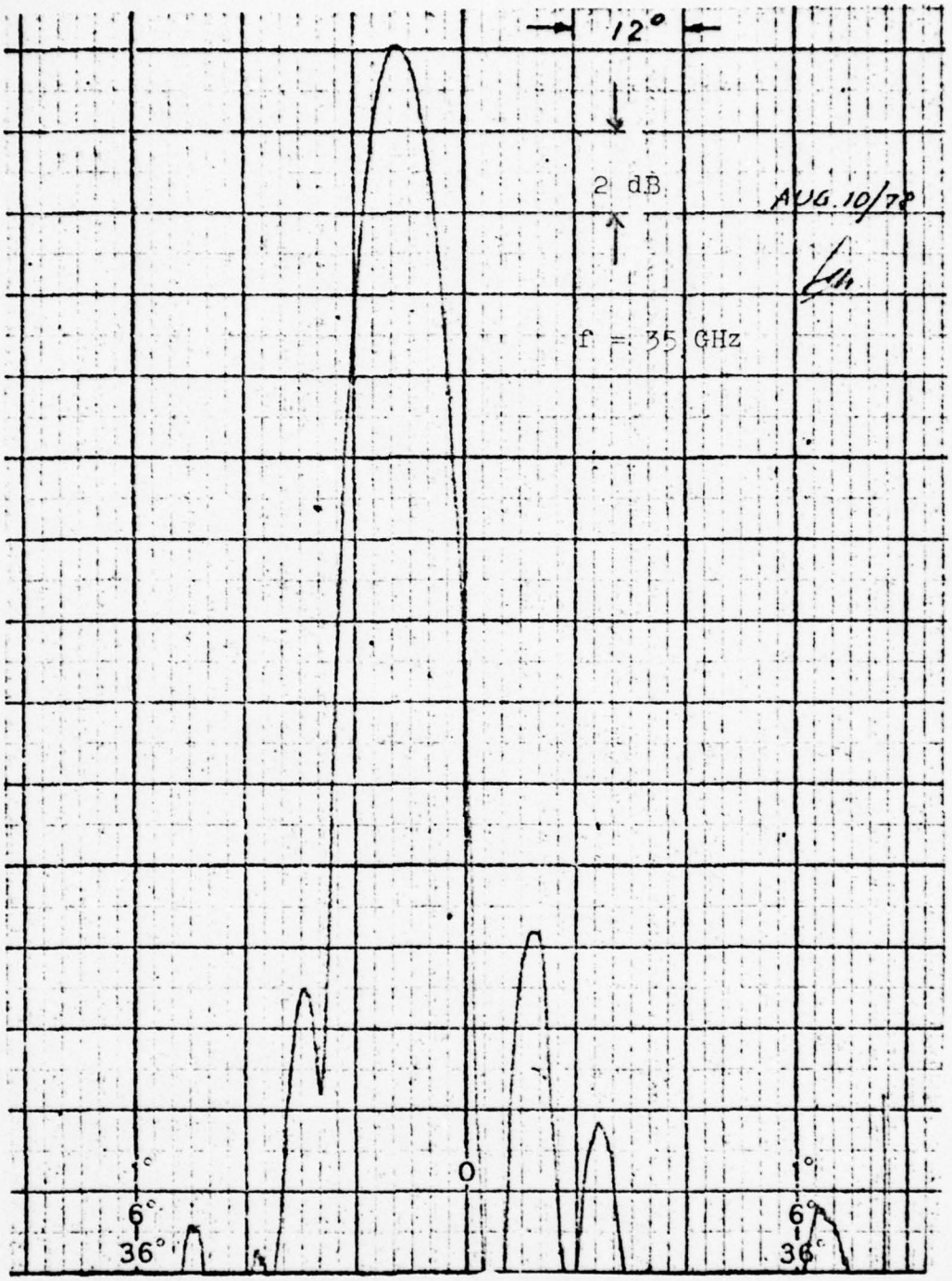

Figure 5-4. Antenna Pattern, E-Plane

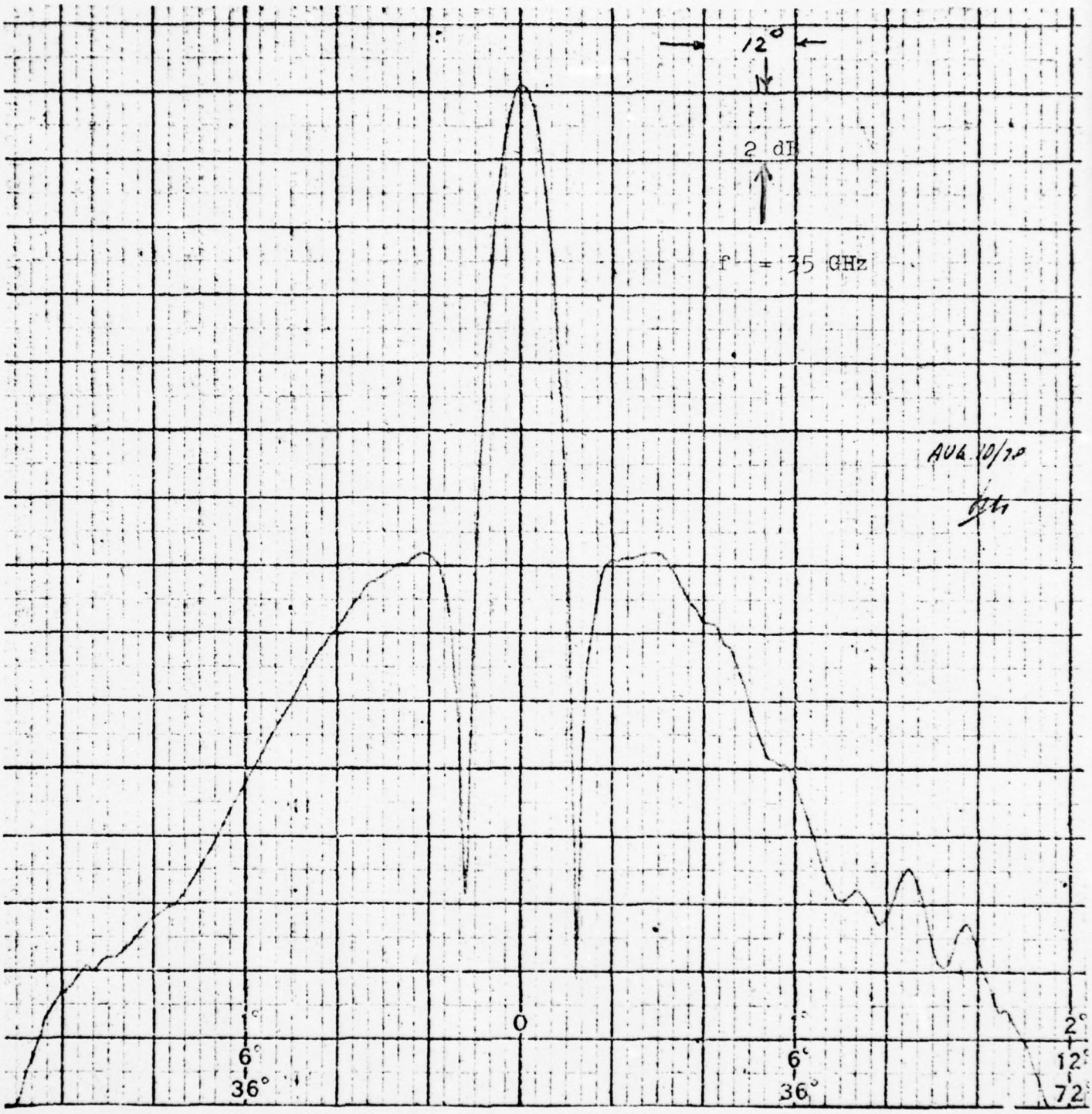

Figure 5-5. Antenna Pattern, H-Plane

E-plane beamwidth:	7°
E-plane beam pointing at center frequency:	7.5° (5 and 10° with mechanical adjustment)
Beam squint with frequency:	Less than 2.5°
H-plane beamwidth:	7°
Beam efficiency:	80 percent
Load power:	5 percent
VSWR:	1.5:1 maximum

5.7 Sensor Configuration

The knowledge and experience acquired during the AIL development of the Radiometer Sensor for STAFF System, Phase I Program under Contract DAAA21-77-R-0019 has been directly applied in developing the STAFF Phase II sensor.

The sensor was designed to provide sufficiently stiff load paths for strength and minimum structural deformation, and to assure a rigid mounting interface. The forward and rear bulkheads are join ed by a set of intersecting longitudinal platforms which support the electronics (see Figure 5-6). In addition, the two pivoted antenna assemblies are locked in position between the bulkheads for additional rigidity.

The sensor assembly, whose total weight is only 3.6 pounds compared to a design goal of 8 pounds, is assembled within the GFE projectile so that the rear bulkhead bottoms on the projectile base thus transferring the set back shock loads to the projectile rear structure. In addition, captivation of the sensor assembly with suitable fastening to the projectile body supports the entire

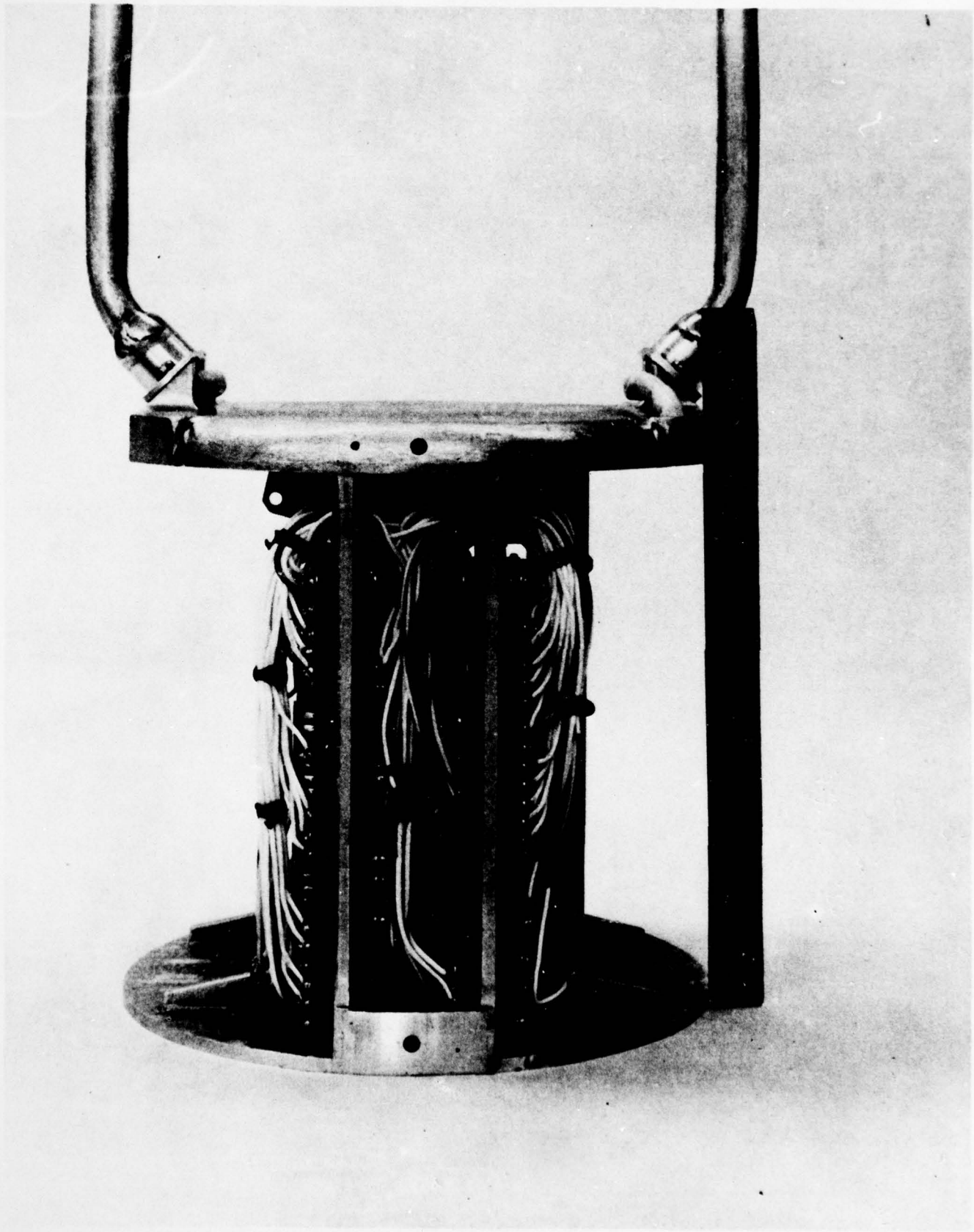

Figure 5-6. Sensor Structure

assembly in an optimum manner for stiffness and strength, thereby ensuring the desired center of gravity (CG) location and dynamic balance of the entire assembly. The sensor and its mating projectile subassemblies are shown in Figure 5-7.

The torque loads developed during spin acceleration are transferred to the warhead mounting as shear loads. Thus high shear strength fasteners are utilized. The longitudinal platform provides mounting surfaces and load paths to the forward and rear bulkheads for the mixer/Gunn diode oscillator assembly, the radiometer receiver assembly, and the signal processor assembly.

Both of the antenna assemblies are pivot mounted with provision for independent orientation to achieve the required squint angle range of from 5 to 10°. In order to minimize any out of plane loads induced by the set back load the antenna feed is nominally designed for a 7.5° squint angle. When the antenna is positioned parallel to the projectile axis, the squint angle is 7.5°, and the antenna assembly will never be tipped more than $\pm 2.5^{\circ}$ from the projectile axis. A short section of flexible waveguide provides the required flexure in the waveguide network.

The mixer/Gunn diode oscillator assembly is located with the projectile spin axis passing through the center of the RF structure (Figure 5-8). This arrangement minimizes the dynamic loads due to the expected spin forces.

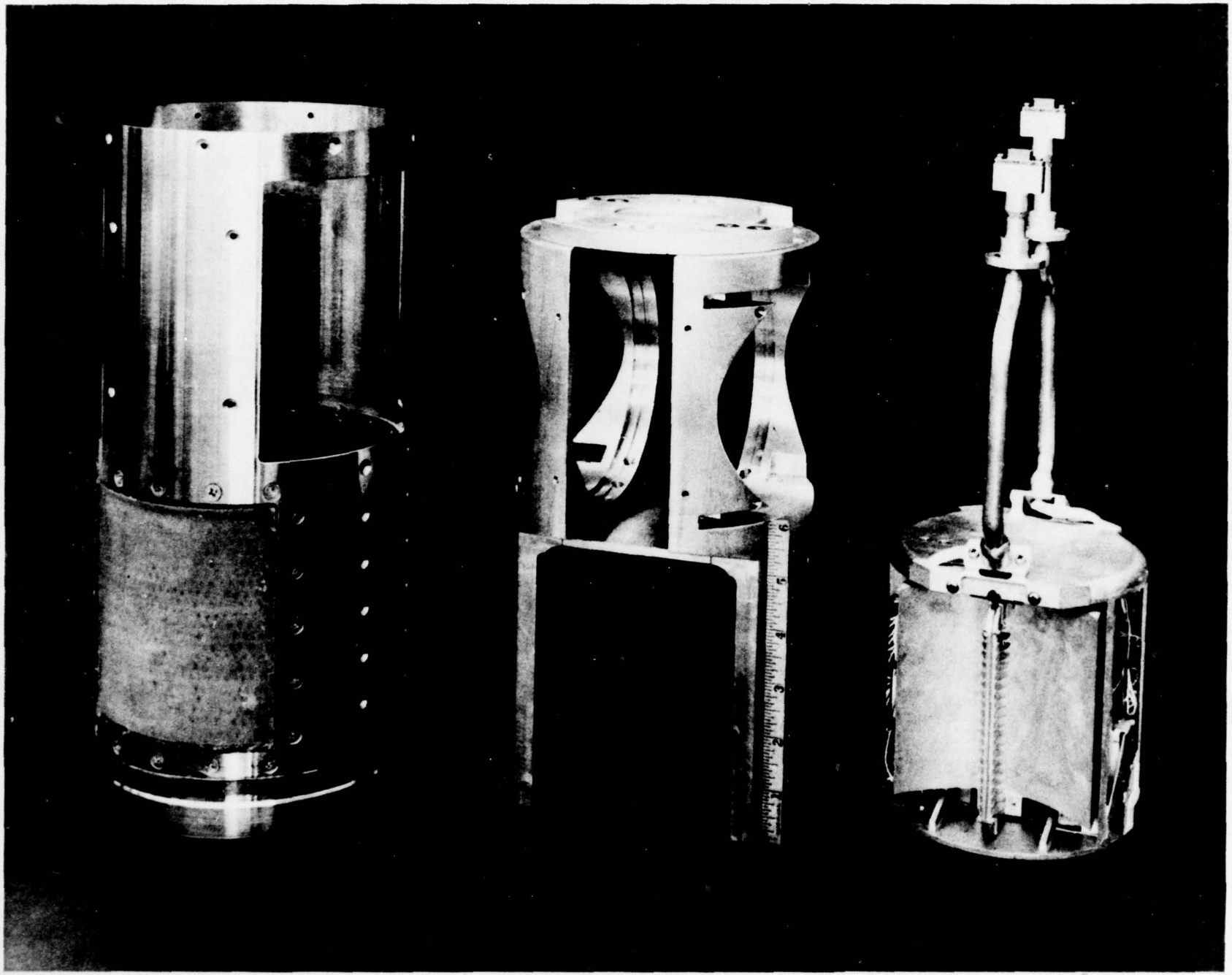

Figure 5-7. Projectile Subassemblies

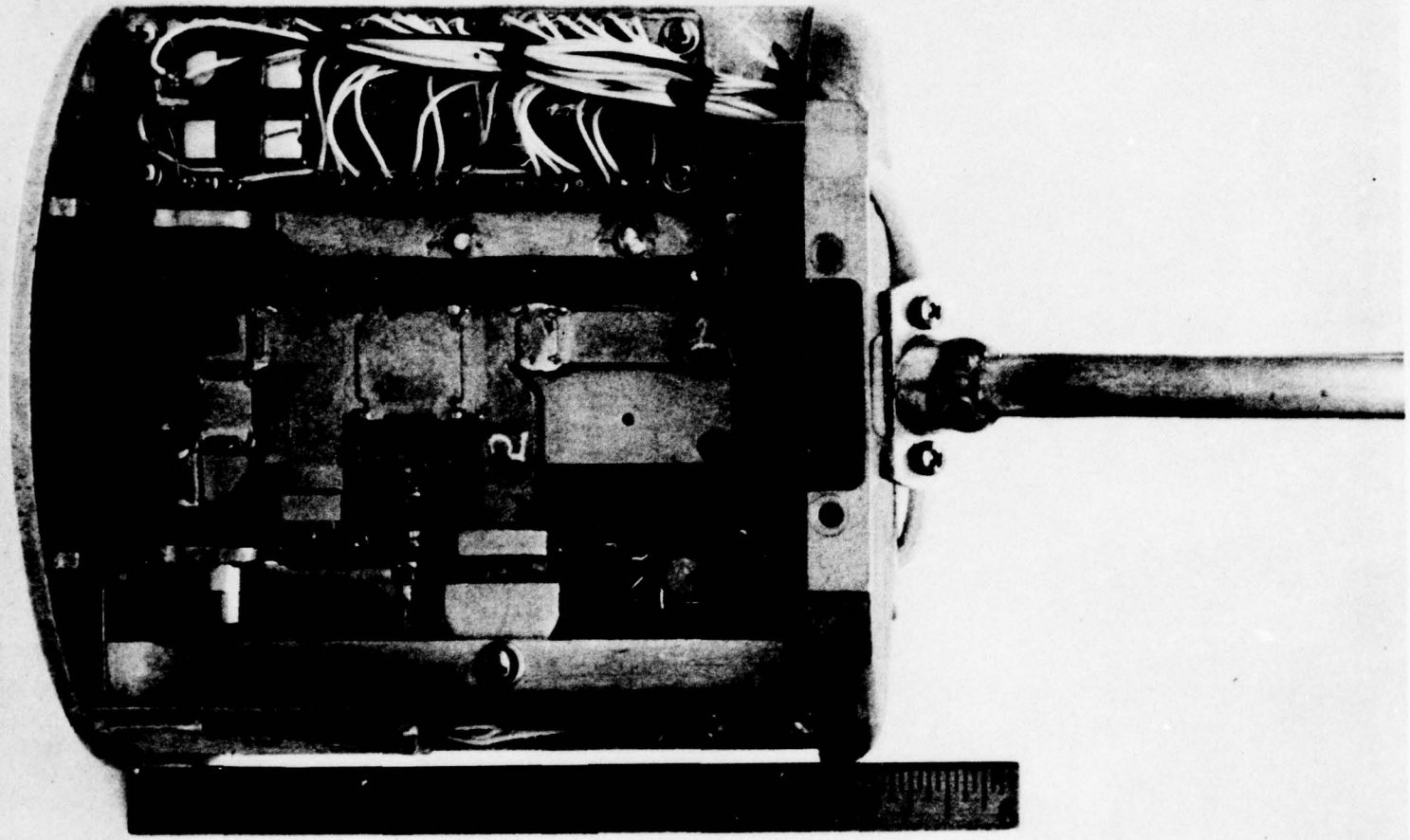

Figure 5-8. RF Structure

The radiometer receiver assembly and the signal processor assembly are printed circuit component card assemblies, and are mounted to the longitudinal platforms. To minimize all loading effects, the boards are mounted in planes which pass as close as practically possible to the spin axis. This arrangement minimizes the induced bending loads and deflections of the printed circuit cards. It should be noted that the individual components on the cards are low in mass, and therefore their CG is relatively close to the card. In view of this consideration, a conformal coating with suitable shear properties is used to transfer component shear loads to the circuit cards. Both the set back loads and the spin loads are transferred using this technique.

The dc power supply is a dual voltage battery within a package which is mounted to the rear bulkhead and designed to operate and survive the induced dynamic loads.

5.8 Analog Processor

The circuit diagram for the AIL analog processor is shown in Figure 5-9. This processor amplifies the detector output in U1A and provides three signal outputs to the digital processor, and four monitor points for telemetry. Positive pulses occur at E4 (antenna sync) each time the antennas view the horizon thus providing pulses at twice the rotation rate so that the projectile spin rate may be measured. A square wave with the same frequency as the spin rate will be present at E5 (antenna phase) to provide the rotation phase that indicates which of the antennas is looking downward.

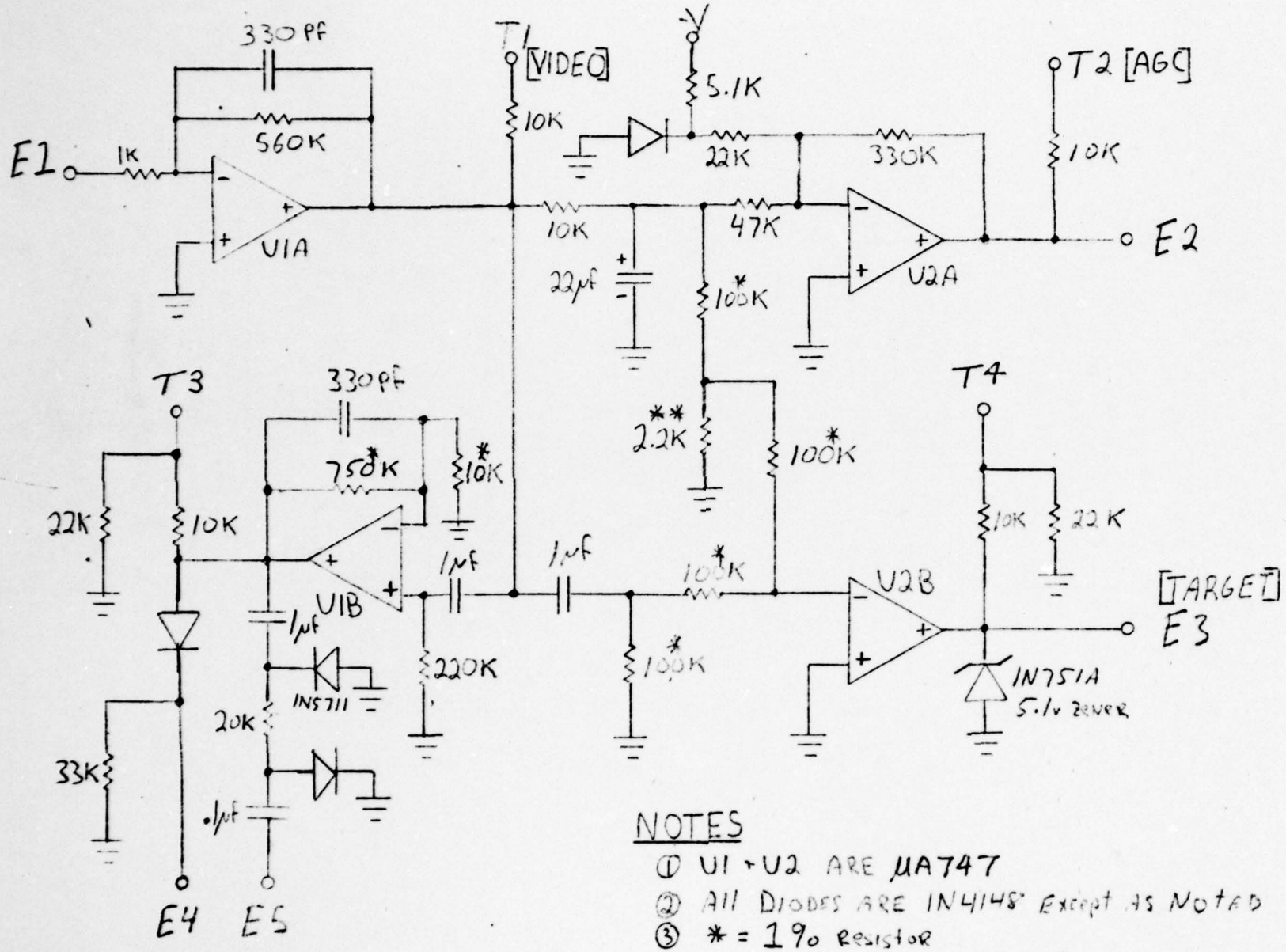

NOTES

① U1 + U2 ARE µA747
② All Diodes are IN4148 Except as Noted
③ * = 1% Resistor
④ ** = SELECT AT TEST
⑤ ALL RESISTORS ARE 1/10 WATT

Figure 5-9. Analog Processor

The amplified voltage from U1A, with average value V_D, provides a threshold reference voltage (KV_D) for the voltage comparator U2B. This amplified detector voltage is filtered by: (a) a lowpass filter with an effective time constant of 0.1 ms, and (b) a highpass filter to reduce the noise content in order to provide a degree of analog pulsewidth discrimination. The scanning of one of the antennas across a target will provide a narrow pulse representing the target's temperature below the background.

The filtered voltage pulse, V_S, produced by this scan will then be compared at U2B with the threshold voltage KV_D. If $V_S > KV_D$, the threshold will be exceeded and the voltage comparator will output a target pulse at E3 during the time that $V_S > KV_D$. Note that the sensor gain will have negligible affect on the target's detection since both V_D and V_S are equally affected by gain.

The processor monitor points and their functions are:

T_1 Video signal

T_2 Average detector level

T_3 Spin rate component

T_4 Target pulses

5.9 Digital Signal Processor

The AIL digital signal processor interprets the output signals from the radiometer receiver and provides the thruster and the munitions "fire" signals in the presence of a valid target. The signal processor detects the target, locates the target center, and triggers one of two thrusters to clear the proper cover from the double ended self forging fragment (SFF) warhead and fires the warhead at the proper time.

The digital processor measures the pulse width and determines if the target signature corresponds to that of an armored vehicle. The processor requires two consecutive detections of the target to fire (i.e., one detection by each of the two antennas). It employs a clock rate technique to derive the time to fire from the target center, and determines which detonator to fire so that the weapon will be directed at the armored target.

5.10 Spin Rate Synchronization Signal

Information indicating the spin rate and the horizon position relative to each sensor system antenna is required in order to accurately define the time delay from target detection that is to be imposed on the firing of the armament as well as which of the two armaments is to be fired

The synchronization signal is extracted from the receiver output using a synchronous detector followed by a lowpass filter with a noise bandwidth of 10 Hz. The resulting radiometer signal-to-noise ratio, conservatively determined from equations (4-2) and (4-5) is:

$$SNR = \frac{T_S}{290 F_S \sqrt{\frac{B_N}{B_{IF}} 8}} \qquad (5\text{-}2)$$

and with: $T_S = 23.9K$
$F_S = 8.0$
$B_{IF} = 500$ MHz
$B_N = 10$ Hz

The SNR is then 25.8 (28 dB) for the phase signal.

5.11 Digital Processor Functions

The following discussion describes the sequence of operations performed by the digital processor (Figure 5-10) during the STAFF projectile's flight.

The antenna sync pulses, with a frequency equal to twice the spin rate, are subjected to a divided by two at FF6 forming logic signal f_s which has a period just equal to the spin rate. Each antenna sync pulse also generates a 1 ms inhibit pulse in mono 1 at the time corresponding to each horizon crossing, as well as an adjustable time pulse T_3 in mono 2. The number of 200 kHz (f_c) clock pulses that occur during one-half of a spin period ($\frac{1}{2f_s}$) less the time T_3 is then counted each revolution by counter U10. The count stored in U10 is therefore $\frac{f_c}{2f_s}(1-2\ f_s\ T_3)$.

When a target pulse is supplied by the analog processor, its duration is compared to a maximum limit in counter U11 and a minimum limit in counter U12. If the target pulse duration is within the specified limits it sets either FF1 or FF2 depending on the phase of the logic signal, f_s. This arms FF3 and FF4 so that a second target pulse will initiate the munitions firing sequence. The occurrence of this first pulse also activates a phase comparison function which analyzes the phases of f_s, the antenna sync phase, and whether FF1 or FF2 was set. The result of this phase comparison performed by U9 and U19 fires thruster A or B, clearing the munition in the proper orientation. Should a second target pulse not occur during the second half of the rotation period all logic functions are reset via U15 (except for the thruster which has already been fired).

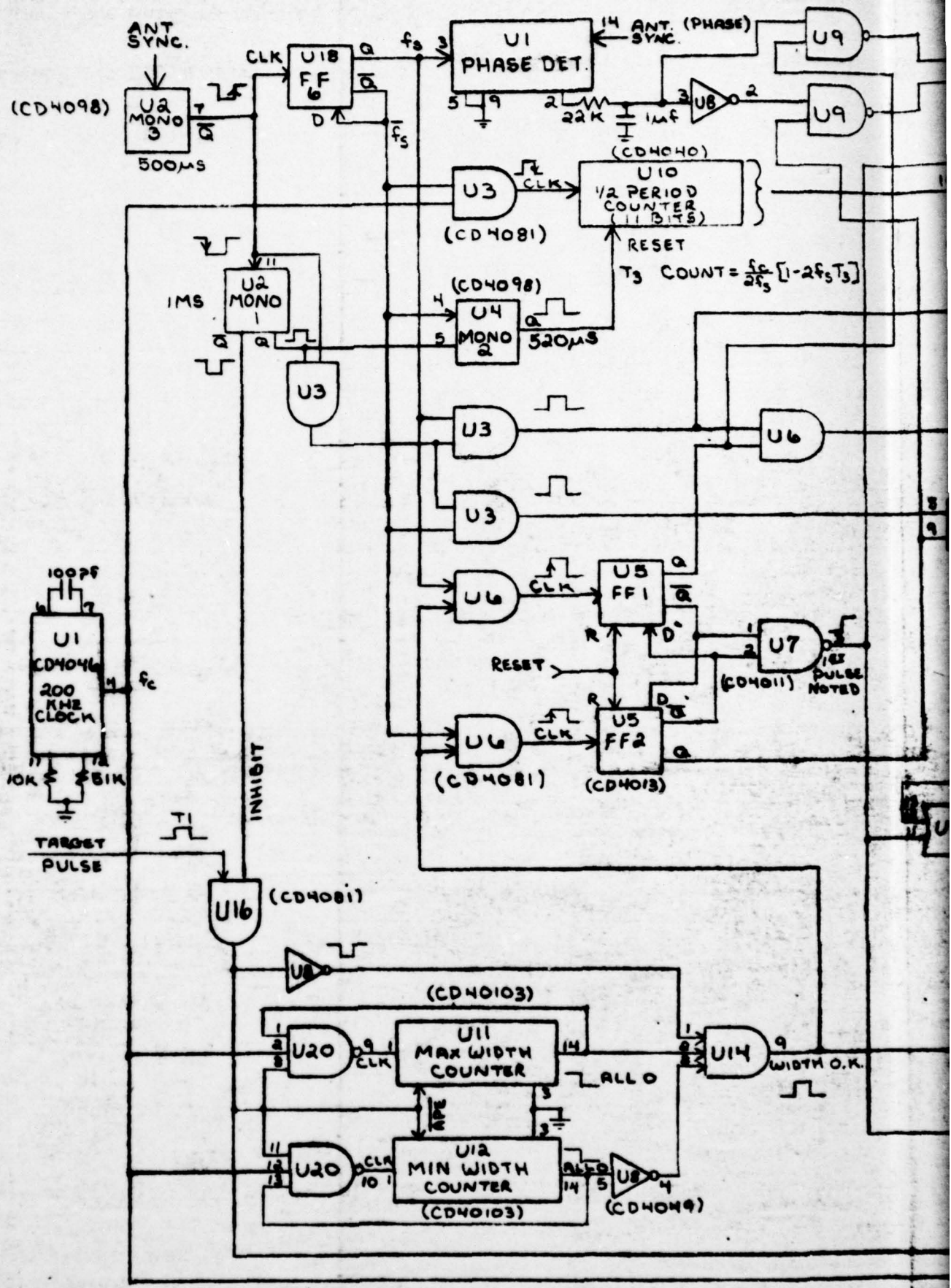
ANT SYNC.
(CD4098)
U2 MONO 3
500μS
CLK
U18 FF 6
D
$\bar{f}_s$
f_s
U1 PHASE DET.
14 ANT. (PHASE) SYNC.
22K
1mf
U8
U9
U9
(CD4040)
U10 1/2 PERIOD COUNTER (11 BITS)
RESET
T_3 COUNT = $\frac{f_c}{2f_s}[1-2f_sT_3]$
U3
(CD4081)
CLK
U2 MONO 1
1MS
(CD4098)
U4 MONO 2
520μS
U3
U3
U6
U3
U6
CLK
U5 FF1
R
D
RESET
U7
(CD4011)
1ST PULSE NOTED
U6
CLK
U5 FF2
(CD4081)
(CD4013)
100pf
U1 CD4046 200 KHZ CLOCK
f_c
10K
51K
INHIBIT
T1
TARGET PULSE
U16
(CD4081)
U8
(CD40103)
U20
CLK
U11 MAX WIDTH COUNTER
ALL 0
U14
WIDTH O.K.
U20
CLK
U12 MIN WIDTH COUNTER
(CD40103)
U8
(CD4049)

FIGURE 5-10

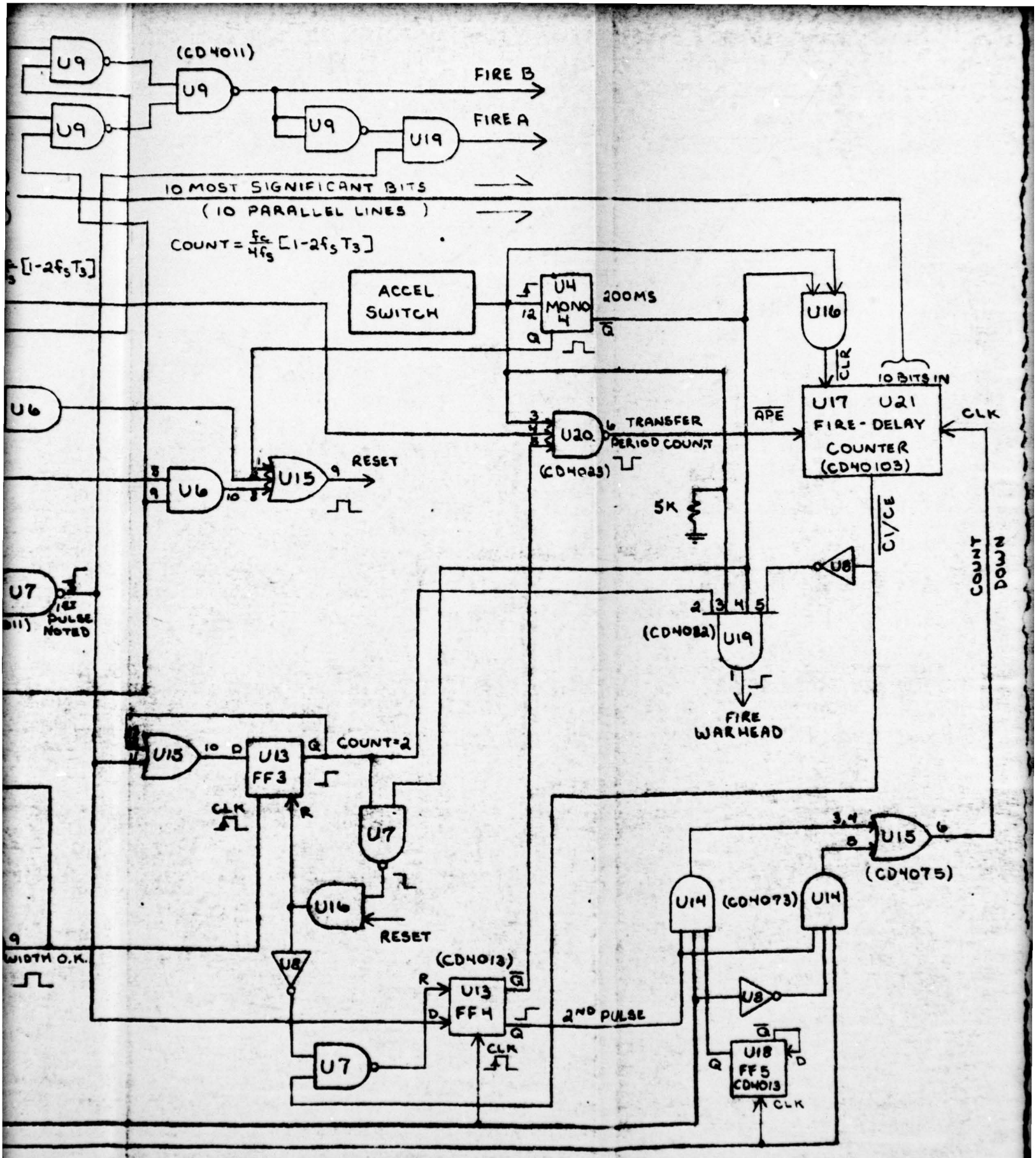

URE 5-10 DIGITAL PROCESSOR

A second target pulse sets FF4 and initiates the munitions firing sequence. This involves transferring one-half of the period count previously stored in counter U10 ($\frac{f_c}{4f_s}[1-2 f_c T_3]$) into count-down counters U17 and U21. These counters are decremented at a rate of $f_c/2$ for the duration of the pulse, T_1, followed by a count-down rate of f_c until their count reaches zero. This operation takes ($\frac{1}{4f_c} - \frac{T_3}{2} + \frac{T_1}{2}$) seconds. Thus a firing delay is imposed which, measured from the leading edge of the target pulse, is one-fourth the rotation period plus one-half the target pulse width minus a predetermined processing delay of $T_3/2$. Should the second pulse not pass the duration test imposed by counters U11 and U12, FF3 will not be set and the fire warhead signal from U19 will be inhibited. System logic reset will then follow.

Firing of the projectile sets an acceleration switch which triggers a 200 ms monostable, mono 4. The logic system is maintained in its reset state during these 200 ms so that both the thrusters and the warhead firing pulses will be inhibited.

5.12 Firing Circuits

The thruster and warhead firing circuits are shown in Figure 5-11.

Transistor Q1 and the transformer form a dc-dc conversion which charges capacitors C1, C2, and C3 to about 150 volts after 1 minute of operation. Turning on of switches SCR 1, 2, or 3 will cause the associated capacitor to discharge through its firing circuit.

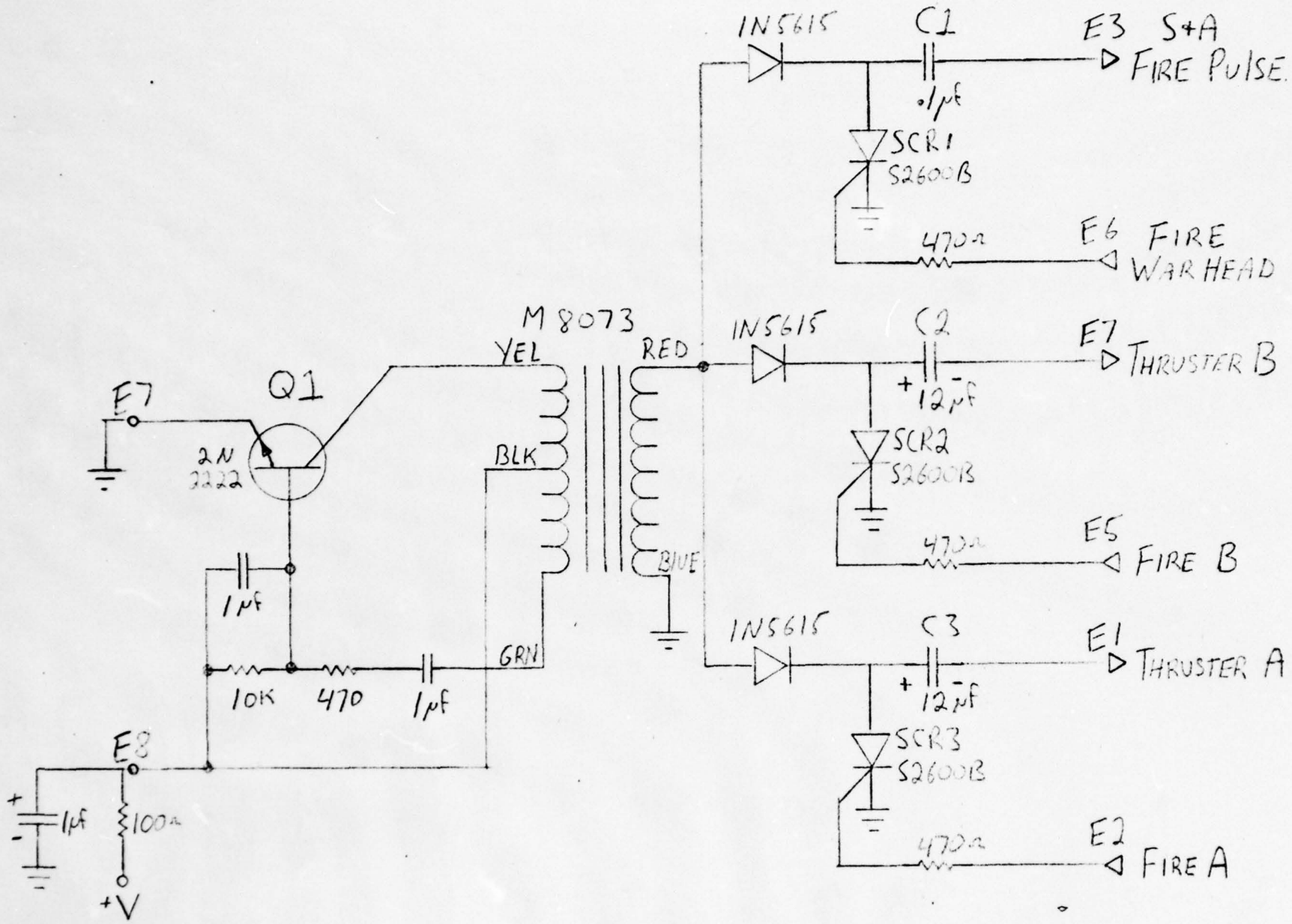

Figure 5-11. Firing Circuits

5.13 Power Requirements

DC power is provided to the sensor by a dual voltage battery composed of five 1/2 amp-hour lithium cells. Two of the cells provide a nominal +5.5 volt battery whose current drain is about 50 mA. A negative 8 volts is provided by the other 3 cells whose current drain is about 200 mA. These batteries power the sensor for a duration in excess of one-half hour.

The GDO device used for the 35 GHz local oscillator requires a regulated -3.9 volt power source. This is provided by the voltage regulator shown in Figure 5-12.

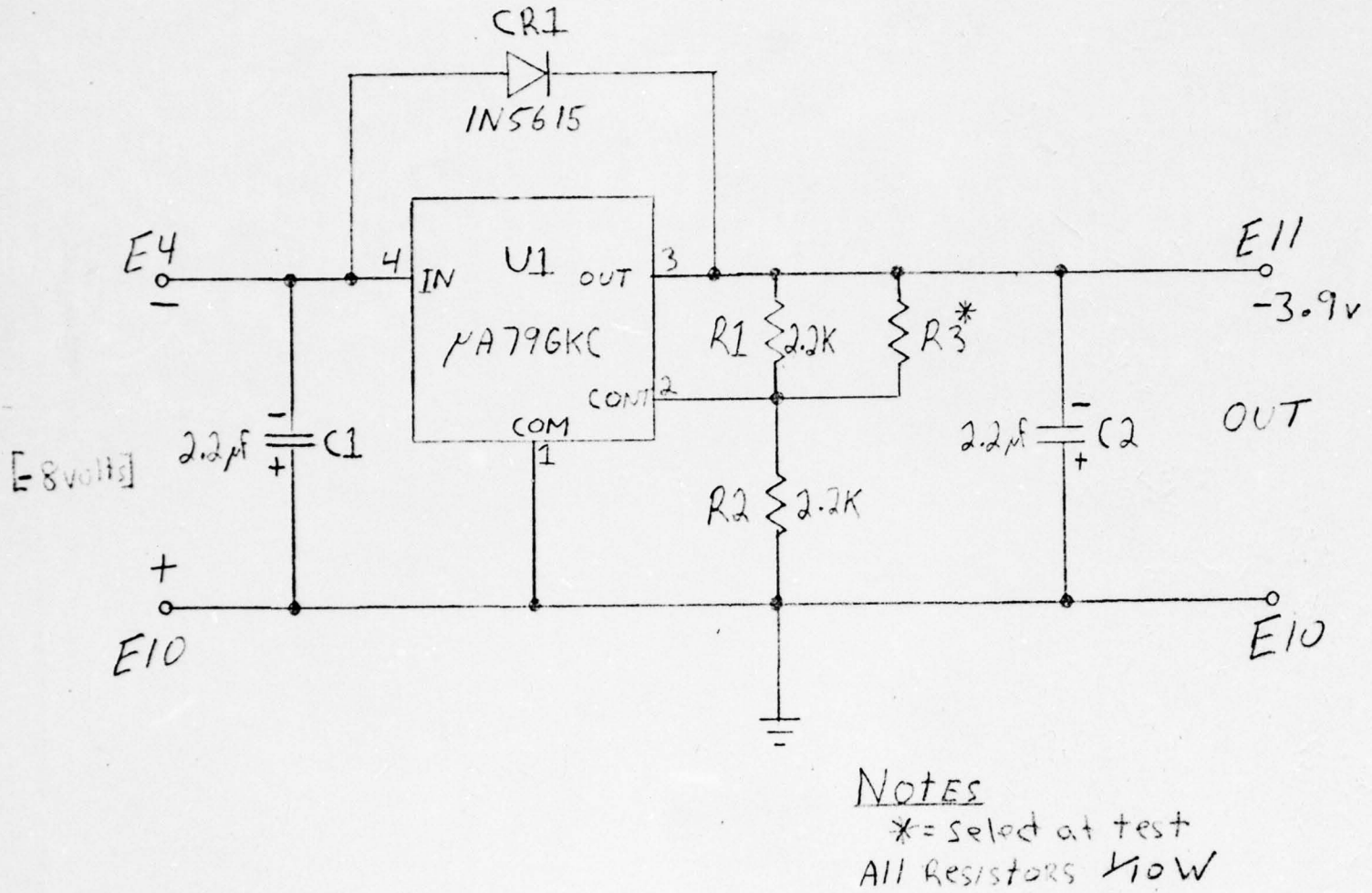

Figure 5-12. Voltage Regulator

6.0 REFERENCES

1. P.H. Deitz, T. Buder, R.A. McGee, "A Computer Simulation of the STAFF Signal Detection and Processing," BRL Interim Memorandum Report No. 558, May 1977.
2. W.B. Davenport, Jr., W.L. Root, "An Introduction to the Theory of Random Signals and Noise," New York, New York: McGraw-Hill, p 253-257, 1958.
3. P.J. Meier, "Integrated Fin-Line and Related Planar Millimeter Circuits," ARPA Millimeter Waves Workshop, NELC (NOSC(, San Diego, Ca., Nov. 1976.
4. J.J. Whelehan, "Low-Noise Millimeter-Wave Receivers," IEEE Trans., Vol. MTT-5, pp 268-280, April 1977.
5. J.A. Calviello, "Mixer and Varactor Diodes," MTT-6 Workshop on Solid-State Millimeter Technology, San Diego, Ca., June 1977. (Update submitted to Sixth ARPA/Tri-Service Millimeter Wave Conference.)
6. "User's Manual for 35 GHz Radiometer AIL Model M105," AIL Division of Cutler-Hammer, Inc., Dept. of Army Contract DAAA21-77-R-0019, May 1977.
7. A. Leber, T. Flattau, P. Meier, "A Low Cost Rugged 35 GHz Tactical Radiometric Sensor," presented at the Sixth ARPA/Tri-Service Millimeter-Wave Conference on 29 Nov. 1977.